

## A Next-Generation High-Speed Data Acquisition System for Multichannel Infrared and Optical Photometry

DAE-SIK MOON, BRUCE E. PIRGER,<sup>1</sup> AND STEPHEN S. EIKENBERRY

Department of Astronomy, Cornell University, Ithaca, NY 14853; moon@astrosun.tn.cornell.edu,  
pirger@astrosun.tn.cornell.edu, eiken@astrosun.tn.cornell.edu

*Received 2000 December 5; accepted 2001 February 7*

**ABSTRACT.** We report the design, operation, and performance of a next-generation high-speed data acquisition system for multichannel infrared and optical photometry based on the modern technologies of field programmable gate arrays, the Peripheral Component Interconnect bus, and the Global Positioning System. This system allows either direct recording of photon arrival times or binned photon counting with time resolution up to 1  $\mu$ s precision in Universal Time, as well as real-time data monitoring and analysis. The system also allows simultaneous recording of multichannel observations with very flexible, reconfigurable observational modes. We present successful 20  $\mu$ s resolution simultaneous observations of the Crab Nebula pulsar in the infrared ( $H$  band) and optical ( $V$  band) wave bands obtained with this system and 100  $\mu$ s resolution  $V$ -band observations of the dwarf nova IY UMa with the 5 m Hale telescope at the Palomar Observatory.

### 1. INTRODUCTION

Real-time, high-speed (microsecond time resolution) data acquisition systems for multichannel infrared and optical photometry have wide potential applications in modern astronomy, not only for scientific observations but also for development of new observational technology. These include observations of compact objects (such as pulsars, X-ray binaries, and cataclysmic variables) (e.g., Eikenberry, Fazio, & Ransom 1996), observations of planetary and lunar occultations (e.g., French et al. 1996; Simon et al. 1999), fringe detection for infrared and optical interferometry (e.g., Mallbet et al. 1999), and wave-front sensing for adaptive optics systems (e.g., Colucci et al. 1994).

Out of the various applications mentioned above, some require precise knowledge of exact Universal Time (UT). For instance, recording of precise UT time is always required in pulsar observations for comparison with the pulse profiles previously obtained and/or obtained from other wavelengths and for studying phase coherence of pulsations. Observations of the planetary and lunar occultations also require the UT time information. In addition, many recent important astronomical discoveries have been possible through the simultaneous multi-wavelength observations (e.g., Eikenberry et al. 1998), which also require precise UT time information for comparison of the data from different observatories. On the other hand, since astronomers use the same telescope, but different detectors, for infrared and optical observations, it is highly desirable that the

data acquisition system is capable of accepting multichannel inputs, allowing simultaneous high-speed photometry in infrared and optical wave bands with the same telescope.

Previous data acquisition systems used for infrared and optical high-speed photometry are typified by the “Li’l Wizard Pulsarator,” built by Richard Lucinio at Caltech and Jerome Kristian at the Carnegie Observatory in the early 1980s. The Wizard has two sets of two counting registers. One register accumulates counts from a detector, while the other counts a preset number of oscillations from a frequency standard. This system is capable of counting photons with time resolution between 5  $\mu$ s and 64 ms and transferring data directly to an Exabyte tape device, along with header information including the number of frequency oscillations since power-up. The Wizard, however, does not allow real-time data monitoring and analysis or direct recording of the UT arrival time of each photon, which makes its applications very limited and inefficient.

The technologies of digital electronics and computer interfaces have developed so fast recently that it is now possible to build an inexpensive next-generation multichannel high-speed data acquisition system which allows real-time data monitoring and analysis as well as direct recording of UT photon arrival times. In this paper we describe the Cornell High-Speed Data Acquisition System (CHISDAS) for multichannel infrared and optical photometry, based on the technologies of field programmable gate arrays (FPGAs), the Peripheral Component Interconnect (PCI), and the Global Positioning System (GPS). Through the FPGA technology, CHISDAS is a fully reconfigurable system, offering very flexible observational modes,

---

<sup>1</sup> Acquisition Systems, Langmuir Lab, Box 1002, 95 Brown Road, Ithaca, NY 14850; <http://www.acsys.com>.

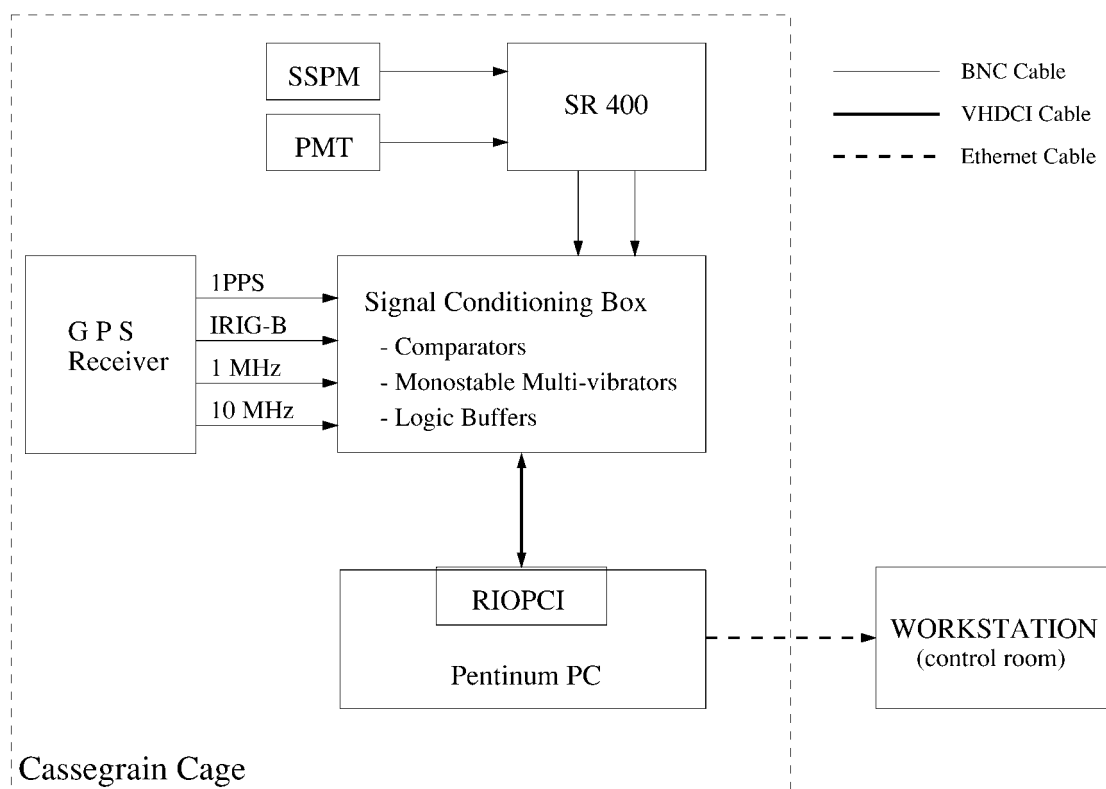


FIG. 1.—A simplified block diagram of CHIDAS in two-channel mode.

including binned counting with time resolution up to  $1 \mu\text{s}$ . Direct recording of the UT arrival time of each photon is also possible up to  $1 \mu\text{s}$  precision by decoding of Inter Range Instrumentation Group Time Code Format B (IRIG-B) signal from a high-precision GPS receiver. CHIDAS is designed to accept signals from up to four data channels simultaneously and can be easily reconfigured to accept signals from more channels.

## 2. HARDWARE AND OVERALL PERFORMANCE

A simplified block diagram of CHIDAS hardware in two-channel mode is shown in Figure 1, where the infrared and optical photometers based on the solid-state photomultiplier (SSPM) and photomultiplier tube (PMT) are used as typical high-speed photometers for the given wave bands, respectively. Analog signals from the photometers are first brought into a Stanford Research SR400 Photon Counter via BNC cables, digitized, and output again via BNC to a signal conditioning box which converts the input signals from the SR400 to TTL digital logic signals. The signal conditioning box also accepts 1 and 10 MHz frequency standards, amplitude modulated IRIG-B signals, and CMOS 1 pulse per second (1PPS) absolute time reference pulses from the GPS receiver. The frequency standards and the IRIG-B signals are converted into TTL pulses in the signal conditioning box. All output signals from the signal

conditioning box are then connected to a data acquisition card inside a Pentium PC through a Very High Density Cable Interconnect (VHDCI) cable.

Figure 2 shows a simplified block diagram of the signal conditioning box. The negative going pulses (from 0 to  $-0.7 \text{ V}$ ) from the SR400 are converted to TTL pulses with a simple comparator circuit (with  $-350 \text{ mV}$  reference level) and a monostable multivibrator. (The monostable multivibrators are used in series with comparators to avoid possible retriggering of the comparators.) The 1 and 10 MHz frequency standards and the IRIG-B signals are converted to TTL pulses in the same way but with reference levels of  $+0$  and  $+1.5 \text{ V}$ , respectively. High-speed logic buffers are finally used to drive all the input signals through the VHDCI cable to the RIOPCI card.

For the data acquisition card, we use the RIOPCI card provided by Acquisition Systems.<sup>2</sup> This card runs on the Windows NT operating system, utilizing an Altera FPGA, high-speed SRAM, an AMCC S5933 ASIC interface to the PCI bus, an integrated daughtercard interface, and a flexible clocking system. The most important part of the RIOPCI card for CHIDAS application is the FPGA, which provides digital logic resources, such as logic gates and registers, that can be interconnected by

<sup>2</sup> <http://www.acqsys.com>.

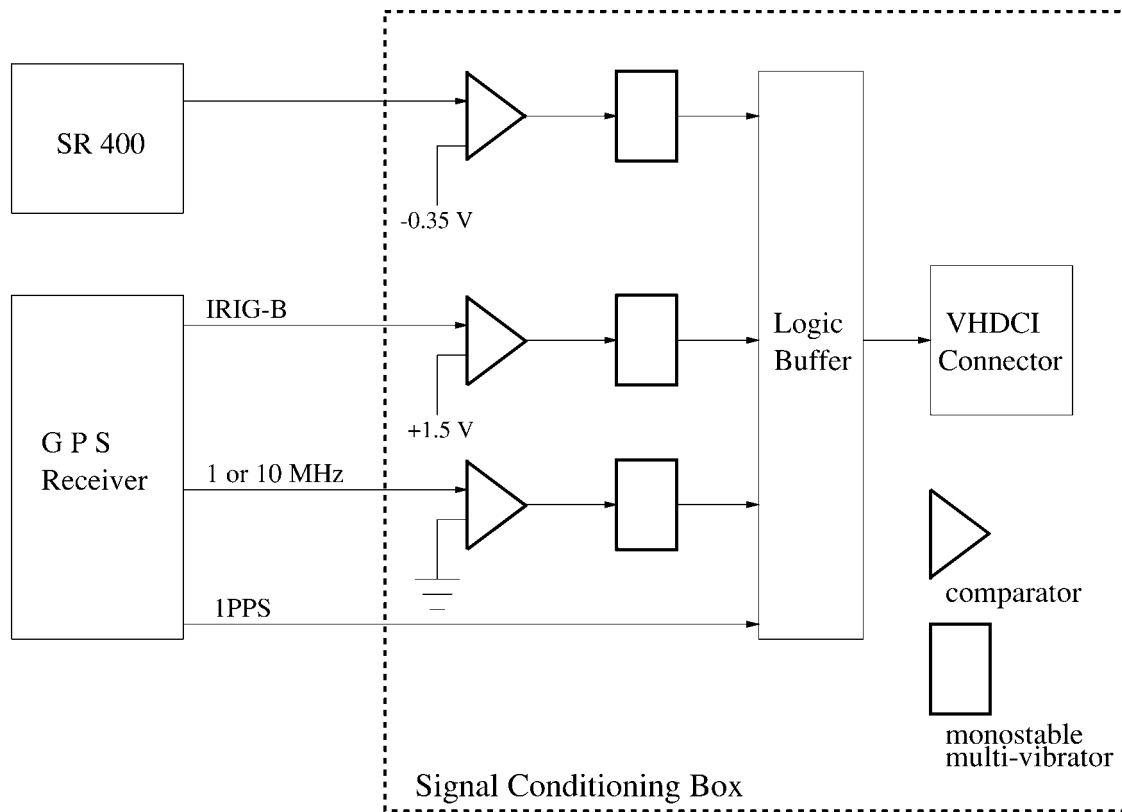


FIG. 2.—A block diagram of signal conditioning box. Simple circuits of comparators and monostable multivibrators are used to convert input analog signals from SR400 and GPS receiver to digital logic signals. Logic buffers are used to drive signals through VHDCI cable.

digital designs to create a digital logic for CHISDAS application. The FPGAs are software configured and can be easily reconfigured to different modes with different digital designs. All of the RIOPCI card resources are available to the end user for custom application development.

The heart of CHISDAS is the digital logic implemented in the FPGA on the RIOPCI card. The digital logic is based on the hierarchical structure of state machines which have several interconnected parts including an interface to the PCI interface, a part for the IRIG-B signal decoding, a multichannel data counter, an interface to the SRAM, and an interface to the daughtercard. The FPGA is first programmed to accept an instruction from the observer through the PCI interface. The instruction is a “double word” (DWORD; a 32 bit digital signal) containing information for UT start time of observations, time resolution, data size for bus-master transfer, and number of input data channels. (The communication between the observer and the FPGA on the RIOPCI card are carried out by C programs interfacing the observer and the registers of the PCI interface. We shall call these C programs “CONTROLLER.” See § 3 for detailed explanations.) In order to start binning of input photon pulses exactly from the given start time of observations, the FPGA is programmed to compare the input IRIG-B signals from the GPS receiver with the given start time

of observations from the instruction DWORD. The photon pulses from the detectors are then binned to the given time resolution with reference to the 1 or 10 MHz GPS frequency standards.

The IRIG-B signal from the GPS receiver is a binary coded decimal amplitude-modulated 1 kHz sine wave. The logic high amplitude is  $+2.5 \pm 0.5$  V while the logic low amplitude is  $+0.75 \pm 0.1$  V. It has information for the exact UT time of the incoming 1PPS pulses. A simple comparator circuit with a monostable multivibrator is used to convert the binary coded decimal wave to TTL pulses. The TTL pulses are then decoded in FPGA programs according to the format of the IRIG-B signal<sup>3</sup> to determine the exact UT time of the incoming 1PPS.

The resulting counted value of each bin is then buffered to the local SRAM in the RIOPCI card. The housekeeping data are also buffered to the local SRAM once per record (one record corresponds to 8192 bins where one bin corresponds to the given time resolution). The housekeeping data are five DWORDs including (1) a security DWORD marking the beginning of the housekeeping data, (2) the instruction DWORD given by the observer, (3) a 40 bit “master counter” value

<sup>3</sup> <http://jcs.mil/RCC/files/200.pdf>.

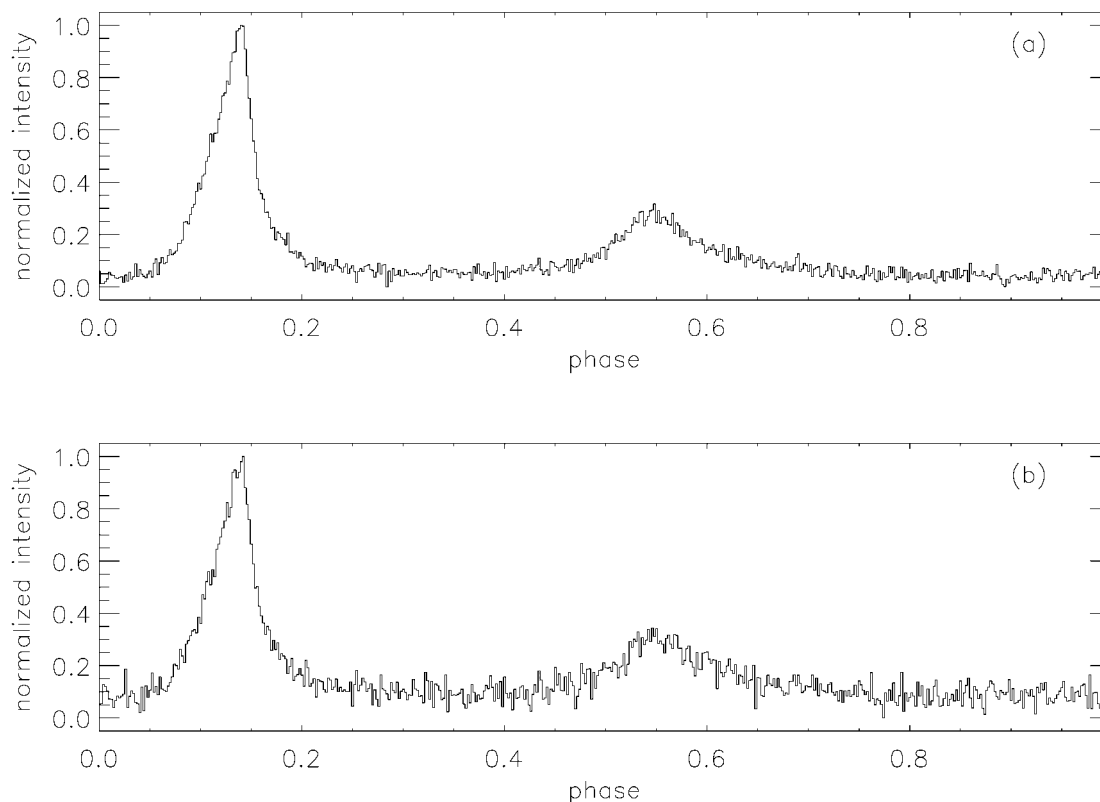


FIG. 3.—(a) Crab Nebula pulsar V-band pulse profile obtained with  $20 \mu\text{s}$  resolution. (b) Same as (a), but for H band. The profiles are obtained simultaneously with  $\sim 4$  hr integration.

clocked by frequency standards from the GPS receiver, (4) a 24 bit “record counter” value, and (5) a 32 bit “bin counter” value. The 40 bit master counter value corresponds to the total integrated frequency standard clocks from the start of observations. The 24 bit record counter value corresponds to the record number from the start of observations, while the 32 bit bin counter value corresponds to the bin number within the given record. The final data are, therefore, a series of 8192 binned values of each record following the housekeeping data of five DWORDs. The buffered data are then directly transferred to the memory of the PC by means of bus-master transfer (i.e., direct memory access). Meanwhile new data are continuously written to the local SRAM in a different SRAM region. The size of each bus-master transfer is given by the observer through the instruction.

Once in PC memory, the CONTROLLER first checks the housekeeping data in order to confirm the continuity of the transferred data. For any incoming errors in the housekeeping data, the CONTROLLER generates error messages and stops operation of the RIOPCI card. After examining the housekeeping data, the CONTROLLER writes the data saved in the PC memory onto a file on local hard disk. It finally transfers the file over an Ethernet connection to the hard disk of the workstation in the telescope control room. The transferred data

are then analyzed by real-time IDL programs on the workstation (we shall call these programs “ANALYZER”; see § 3) and recorded on tapes for storage.

### 3. SOFTWARE

The CHISDAS software consists of two parts: the CONTROLLER on the PC and the ANALYZER on the workstation.

Three main functions of the CONTROLLER are (1) controlling the PCI interface on the RIOPCI card to configure the FPGA, to give instructions to the FPGA through the FIFO, and to save the transferred data, via bus-master transfer from the FPGA, in the PC memory; (2) monitoring the incoming housekeeping data to examine the operation of the CHISDAS; and (3) transferring the data in PC memory to the hard disk on the workstation in the telescope control room through an Ethernet connection.

ANALYZER includes programs for (1) plotting photon counts per second for the real-time monitoring of the incoming data, (2) making time series from the raw data and rebinning the time series, and (3) performing fast Fourier transformation (FFT) and power spectrum analysis. It also includes several advanced programs especially useful for pulsar observations, such as routines for (1) barycentering the time series using the

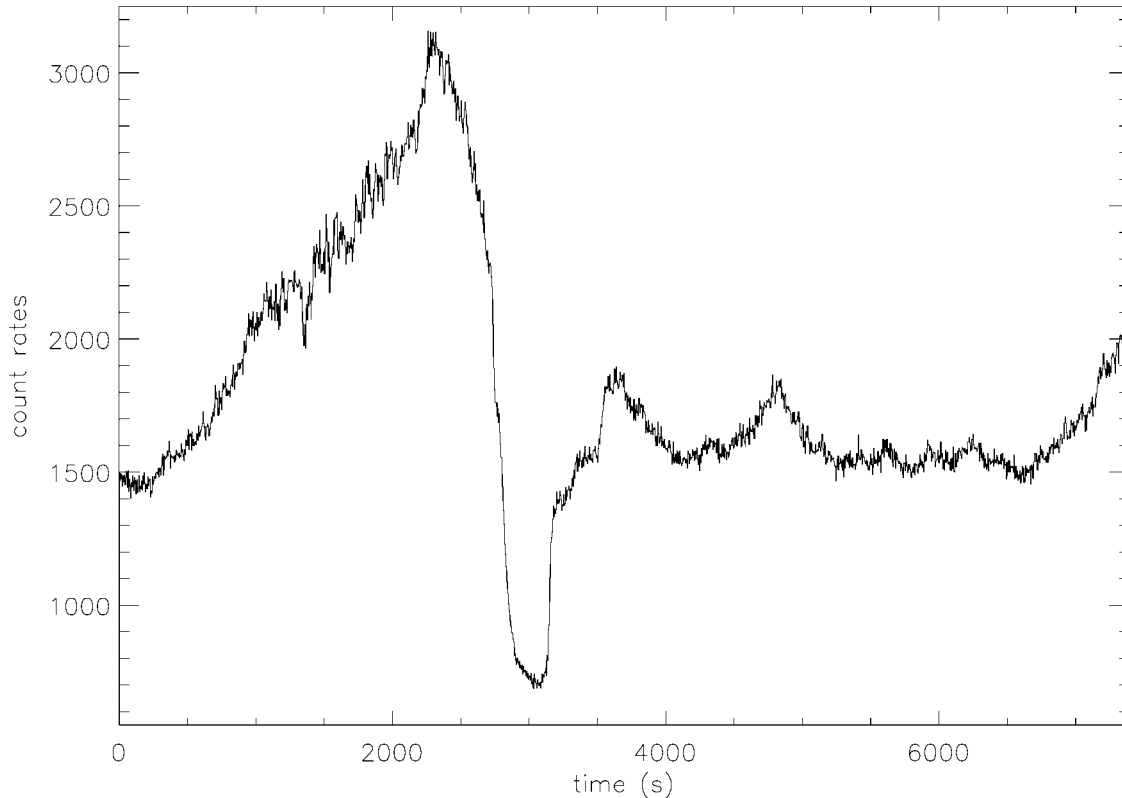


FIG. 4.—V-band light curve of the dwarf nova IY UMa obtained by binning the 100  $\mu$ s raw data to 4.096 s resolution.

JPL 200 ephemeris based on TEMPO,<sup>4</sup> (2) Fourier interpolation (Eikenberry 1997), (3) signal-folding in order to find frequency and its derivative (Eikenberry 1997), and (4) generating pulse profiles.

#### 4. OBSERVATIONAL EXAMPLES

CHISDAS has been successfully used with infrared and optical high-speed photometers based on SSPM and PMT on the 5 m Hale telescope of the Palomar Observatory for various sources including pulsars, X-ray binaries, and cataclysmic variables. Two examples of the observations with CHISDAS are given here. One is 20  $\mu$ s simultaneous infrared and optical wave band observations of the Crab Nebula pulsar, which is specifically based on CHISDAS capability of multichannel observations and direct recording of UT time. (Note that the *Unconventional Stellar Aspect [USA]* X-ray satellite [Ray et al. 1999], which has an onboard GPS receiver, was used together for simultaneous infrared, optical, and X-ray observations.) The other is 100  $\mu$ s V-band observations of the eclipsing dwarf nova IY UMa (Uemura et al. 2000), for which the  $\sim 10^2$  s timescale variability of the source (such as eclipse and humps)

was well traced in real time owing to the real-time monitoring capability of CHISDAS.

Figure 3 shows the  $\sim 4$  hr infrared (*H* band) and optical (*V* band) pulse profiles of the Crab Nebula pulsar obtained by the two-channel mode photometry with 20  $\mu$ s resolution on 1999 November 28.

The observed data were analyzed with ANALYZER. First, the photon arrival times from the raw data were transformed to the solar system barycenter using the JPL DE200 ephemeris. The barycentered time series was then rebinned to 2.56 ms resolution. The maximum power frequency was found to be  $f_{\max} \approx 29.847194$  Hz through the FFT of the binned time series. The routines for the Fourier interpolation and signal folding were used to find the signal-folded frequency of  $f_{\text{sf}} \approx 29.8472(1)$ .<sup>5</sup> During the signal folding, the frequency derivative was fixed to be the value,  $f \approx -3.7461751 \times 10^{-10} \text{ s}^{-2}$ , of the monthly Jodrell Bank radio ephemeris.<sup>6</sup> The signal-folded frequency is in good agreement with the Jodrell Bank radio frequency of  $f_r \approx 29.8472117964(2)$ . Finally, the pulse profiles in Figure 3 were obtained using the Jodrell Bank ephemeris. This is the

<sup>4</sup> <http://pulsar.princeton.edu/tempo>.

<sup>5</sup> The value in parentheses is the 1  $\sigma$  uncertainty in the last quoted digit.

<sup>6</sup> <http://www.jb.man.ac.uk/~pulsar/Resources/resources.html>.

first ever, as far as we are aware, simultaneous photometry in infrared and optical wave bands with high time resolution. A full analysis of the data will be presented elsewhere with the data of the *USA* X-ray observations.

Figure 4 shows the *V*-band light curve of the dwarf nova IY UMa, of which the orbital period is  $\sim 1.77$  hr (Uemura et al. 2000). The  $100 \mu\text{s}$  resolution raw data were binned to 4.096 s resolution, and we can clearly identify several features including a gradual rise before the eclipse, a deep eclipse, and two post-eclipse superhumps. These are unique observations providing detailed information of the source, since the previous studies rely on the observations with small telescopes (e.g., 40 cm aperture) and with poor time resolutions (e.g. 30 s), which make it impossible to study the source in detail (see Uemura et al. 2000). A full analysis of the data will be presented elsewhere.

## 5. CONCLUSIONS

We have described a next generation high-speed data acquisition system for multichannel infrared and optical photom-

etry. CHISDAS opens a new window for high-speed infrared and optical photometry in many ways. Among them are (1) real-time data monitoring and analysis, (2) direct recording of UT photon arrival times, (3) simultaneous observations in multichannels, and (4) full reconfigurability of the system. CHISDAS has already proved to be very powerful and successful in real observations, and will be used widely for high-speed infrared and optical photometry.

We would like to thank the referee and editor for comments and suggestions which simplified the appearance of this paper. We thank Justin Schoenwald for his help on the AMCC S5933 PCI device driver from Acquisition Systems. We also thank Chuck Henderson and Craig Blacken for their help in building the signal conditioning box. We finally thank the staff members of the Palomar Observatory for their help on our observations. D. S. M. is supported by NSF grant AST 99-86898. S. E. E. is supported in part by an NSF Faculty Early Career Development (CAREER) award (NSF-9983830).

## REFERENCES

- Colucci, D., Lloyd-Hart, M., Wittman, D., Angel, R., Ghez, A., & McLeod, B. 1994, *PASP*, 106, 1104  
 Eikenberry, S. S. 1997, Ph.D. thesis, Harvard Univ.  
 Eikenberry, S. S., Fazio, G. G., & Ransom, S. M. 1996, *PASP*, 108, 939  
 Eikenberry, S. S., Matthews, K., Morgan, E. H., Remillard, R. A., & Nelson, R. W. 1998, *ApJ*, 494, L61  
 French, R. G., et al. 1996, *Icarus*, 119, 269  
 Mallbet, F., Kern, P., Schanen-Duport, I., Berger, J.-P., Rousselet-Perraut, K., & Benech, P. 1999, *A&AS*, 138, 135  
 Ray, P. S., et al. 1999, preprint (astro-ph/9911236)  
 Simon, M., Beck, T. L., Greene, T. P., Howell, R. R., Lumsden, S., & Prato, L. 1999, *AJ*, 117, 1594  
 Uemura, M., et al. 2000, *PASJ*, 52, L15